



Purification, cloning and characterization of fragaceatoxin C, a novel actinoporin from the sea anemone *Actinia fragacea*

Augusto Bellomio¹, Koldo Morante, Ariana Barlič², Ion Gutiérrez-Aguirre³, Ana Rosa Viguera, Juan Manuel González-Mañas*

Unidad de Biofísica (Centro Mixto CSIC-UPV/EHU) and Departamento de Bioquímica, Universidad del País Vasco, Aptdo. 644, 48080 Bilbao, Spain

ARTICLE INFO

Article history:

Received 25 March 2009

Received in revised form 16 June 2009

Accepted 19 June 2009

Available online 27 June 2009

Keywords:

Fragaceatoxin C

Actinoporins

Lipid-protein interactions

ABSTRACT

Actinia fragacea is commonly called the “strawberry” anemone because of the distinctive yellow or green spots displayed on its red column. Its venom contains several haemolytic proteins with a molecular mass of ~20 kDa that can be separated by ion-exchange column chromatography. One of them was purified to homogeneity and was named fragaceatoxin C (FraC). Its 15 N-terminal residues were identified by Edman degradation and served to obtain its complete DNA coding sequence by RT-PCR. The coding region of FraC was amplified and cloned in the expression vector pBAT-4. Purified recombinant FraC consists of 179 amino acids and multiple sequence alignment with other actinoporins clearly indicates that FraC belongs to this protein family. The secondary structure, thermal stability and lytic activity of native and recombinant FraC were practically identical and exhibit the same basic features already described for equinatoxin-II and sticholysin-II.

© 2009 Elsevier Ltd. All rights reserved.

1. Introduction

Sea anemones of the genus *Actinia* are very common in the intertidal zone of the northern rocky coast of Spain facing the Cantabrian Sea and the Bay of Biscay. *Actinia equina* is one of the most abundant species and shows a high degree of polymorphism: specimens with green, brown, red and striped or spotted columns can be observed. Initially considered as a morphological variant of *Actinia equina*, *Actinia fragacea* raised its status to specific

level after the work of Carter and Thorpe (1981), who demonstrated that both species were genetically different. *A. fragacea* is also known as the “strawberry” anemone because of the yellow or green spots displayed on its red column. In contrast to *A. equina*, *A. fragacea* is larger (up to 10 cm in diameter), lacks viviparity (Perrin et al., 1999) and is most often found solitary (Walton, 1911).

Sea anemones produce two types of protein toxins: neurotoxins, which act mainly on ion channels (Honma and Shiomi, 2005) and cytolytins (or actinoporins), which exhibit lytic activity on a variety of cells (Anderluh and Maček, 2002; Alegre-Cebollada et al., 2007a; Álvarez et al., 2009; Kristan et al., 2009). The isolation and characterization of haemolytic toxins from the venom of *Actinia fragacea* results interesting for a number of reasons. Our main goal is to determine if they share the main features of the anemone_cytotox protein family, which is stored in the Pfam database (Finn et al., 2008) under the code number PF06369. By expanding the family, sequence comparison might help to identify the key amino acid residues involved in the mechanism of

* Corresponding author. Tel.: +34 94 601 5379; fax: +34 94 601 3500.

E-mail address: juanmanuel.gonzalez@ehu.es (J.M. González-Mañas).

¹ Present address: Instituto de Química Biológica, Facultad de Bioquímica, Química y Farmacia, “Dr. Bernabé Bloj” and Instituto Superior de Investigaciones Biológicas (INSIBIO), Departamento de Bioquímica de la Nutrición (CONICET-UNT), Chacabuco 461, San Miguel de Tucumán, T4000ILH Tucumán, Argentina.

² Present address: Educell, d. o. o., Šljajmerjeva 6, SI-1000 Ljubljana, Slovenia.

³ Present address: Department of Plant Physiology and Biotechnology, National Institute of Biology, Večna pot 111, SI-1000 Ljubljana, Slovenia.

pore formation and the effects of their replacement. Next, we will try to determine their primary structure by cloning techniques.

In the present work we describe the purification, cloning and characterization of a novel haemolytic toxin extracted from the venom of *Actinia fragacea*. Its primary structure shares, at least, 55% identity and 76% similarity with other actinoporins. Structural and biochemical characterization were carried out for both, the native and the recombinant proteins. Circular dichroism experiments show that both proteins are composed mainly of β -structure. Their interaction with cell and model membranes is practically identical and resembles that of equinatoxin-II and sticholysin-II. The successful cloning, expression and purification of this toxin will pave the way for the design of different mutants for structural and/or functional studies. We propose the term fragaceatoxin C (FraC) to name it.

2. Materials and methods

2.1. Materials

Egg phosphatidylcholine (PC) and bovine brain sphingomyelin (SM) were from Avanti Polar Lipids (Alabaster, AL, USA). 8-Aminonaphthalene-1,3,6-trisulfonic acid (ANTS) and *p*-xylene-bis-pyridinium bromide (DPX) were from Molecular Probes, Inc. (Eugene, OR, USA). Triton X-100 was from Sigma (St. Louis, MO, USA). The restriction enzymes NcoI and HindIII were from Roche (Basel, Switzerland), the *Pfu* Turbo DNA polymerase was from Stratagene (California, CA, USA) and the ligase was from New England Biolabs (UK).

2.2. Collection of anemones

Specimens of *A. fragacea* were collected in the northern coast of Spain, facing the Cantabrian Sea. Anemones were carefully detached from the rocky substrate to avoid cell rupture and deposited in a glass beaker surrounded by ice. Accumulation of the animals generated enough stress as to induce venom release. After collecting about 50 specimens, the volume of the exuded liquid was approximately 200 ml. Anemones were further squeezed through a nylon membrane to extract the maximum volume of liquid and thrown back to the sea.

2.3. Purification of the native toxins

The initial extract was centrifuged at $20,000 \times g$ for 30 min at 4 °C in an Avanti™ (Beckman Coulter, USA) centrifuge to pellet down the solid bodies and cellular debris. Fifty ml aliquots of the supernatant were taken, frozen in liquid nitrogen and stored at –26 °C until needed. An aliquot of the initial extract was thawed in a water bath at room temperature and milliQ water was added to obtain a final volume of 500 ml. The diluted sample was filtered through a Nylafo™ filter (Pall Life Sciences, NY, USA) with a pore diameter of 0.45 μ m and the filtrate was applied to a SP-Sepharose™ Fast Flow (Amersham Biosciences, GE healthcare, UK) cationic-exchange chromatography column (20×2.5 cm) connected to an ÄKTA™ FPLC chromatographic

System (GE Healthcare, UK). The chromatography column was equilibrated with milliQ water and eluted with a step NaCl gradient (Elution buffer A was 50 mM sodium phosphate, pH 7.5 and elution buffer B was 0.7 M NaCl, 50 mM sodium phosphate, pH 7.5). The elution started with 5% buffer B for the first 50 ml and its proportion was raised to 21%, 42%, 62% and 100% after every 100 ml of elution volume. Twelve ml fractions were collected and assayed for haemolytic activity and protein content by SDS-PAGE (see below). Fractions associated to each haemolytic peak were desalted and concentrated by means of an Amicon® Ultra filter (Millipore Corporation, USA) with a molecular weight cut-off (MWCO) of 10,000 Da.

2.4. Purification of fragaceatoxin C

The concentrated fractions containing fragaceatoxin C (second haemolytic peak in the first chromatography) were further purified. A total of 500 μ l of the concentrated protein solution were applied to a Mono S® HR 5/5 column (Pharmacia Biotech, Uppsala, Sweden) equilibrated with 50 mM sodium acetate buffer, pH 5 (buffer A). Buffer B was 1 M NaCl, 50 mM sodium acetate buffer, pH 5. The elution was carried out with a linear gradient between 0.4 M and 0.9 M NaCl. Fractions corresponding to the single haemolytic peak were concentrated and desalted with an Amicon® Ultra filter (MWCO = 10,000 Da) and stored at –26 °C until needed. Protein concentration of the purified fragaceatoxin C was determined from its absorbance at 280 nM, using a molar extinction coefficient (ϵ) of $42,530 \text{ M}^{-1} \text{ cm}^{-1}$ (Gill and von Hippel, 1989).

2.5. Protein electrophoresis

SDS-PAGE was carried out as described by Laemmli (1970). Protein staining was carried out either with Silver Stain Plus Kit (Bio-Rad Laboratories, Inc., USA) or with Coomassie dye. Low-range molecular weight markers (Bio-Rad Laboratories Inc., USA) were used as reference.

2.6. Haemolytic activity

Sheep red blood cells (Biomedics, Alcobendas, Spain) were extensively washed with 150 mM NaCl, 5 mM sodium phosphate, pH 8 buffer until the supernatant was clear. The erythrocytes were resuspended in the same buffer and the A_{700} was adjusted to 0.6. Haemolytic activity was assayed by monitoring the changes in turbidity (A_{700}) in a Cary 3 spectrophotometer (Varian, Australia) (Louw and Visser, 1977). Haemolytic activity is expressed as the inverse of $T_{1/2}$, which is the time (in seconds) needed to achieve 50% of the initial absorbance.

To determine the dependence of haemolytic activity on toxin concentration we carried out 2-fold serial dilutions of native and recombinant FraC in a 96-well titration plate with 150 mM NaCl, 5 mM sodium phosphate buffer, pH 8. After the dilutions, the volume of each toxin solution was 100 μ l. To each well, 100 μ l of a suspension of sheep erythrocytes were added. After an incubation period of 90 min at room temperature A_{412} was measured in

a Biomate 3 spectrophotometer (Rochester, NY, USA). Percentage haemolysis was calculated as follows:

$$\%haemolysis = 100 \times [(A_{fin} - A_{min}) / (A_{max} - A_{min})]$$

where A_{fin} corresponds to the final absorbance measured for each well. A_{max} and A_{min} represent the A_{412} values for haemolysed (added to milliQ water) and intact (added to buffer) red blood cells, respectively.

2.7. N-terminal amino acid sequence determination

SDS-PAGE protein bands corresponding to the haemolytic peaks obtained in the first chromatographic step were transferred to a polyvinylidene fluoride (PVDF) membrane (Immobilon-P Millipore) by means of a Trans-Blot[®] SD semi-dry electrophoretic transfer cell (Bio-Rad Laboratories, Inc., USA). The membrane was immersed in methanol and stained with 0.1% Coomassie in water/methanol/acetic acid (60/39/1) to identify the proteins of interest. The membranes were allowed to dry at room temperature and the bands with a molecular weight of ~20 kDa were excised to have their 15 N-terminal residues sequenced by the Edman degradation method (Edman and Begg, 1967) with an Applied Biosystems Procise 494 protein sequencer (Foster City, CA, USA).

2.8. Cloning and determination of the sequence

RNA was obtained from a single specimen of *A. fragacea* following the protocol described by Chomczynski and Sacchi (1987) and used as a template for the synthesis and amplification of cDNAs coding for actinoporins using a Qiagen OneStep RT-PCR Kit following the manufacturer's instructions. Two forward primers were used: ol_fra1 and ol_fra3b, designed after N-terminal sequencing of the haemolytic proteins. The reverse primer was ol_pTb and was designed to hybridize with the polyA tail of mRNAs (see Table 1). cDNAs with a size of ~750 base pairs were selected for cloning in a pGEM[®]-T Easy Vector for PCR products (Promega, Madison) (Clark, 1988). Plasmid DNA preparation, digestions, ligations, transformations, and electrophoresis were done by standard methods (Sambrook and Russel, 2001). The ligation mixture was used to transform the *E. coli* XL1-Blue strain. The presence of an insert within the vector results in the bluish or white color of the colonies grown in LB solid medium containing X-Gal and ampicillin and was further confirmed by restriction analysis and DNA sequencing of the selected plasmids.

2.9. Expression and purification of recombinant fragaceatoxin C

The fragaceatoxin C coding sequence was amplified by PCR with forward ol_FraERBS2 and reverse ol_Fra1d primers (see Table 1). The reaction was carried out using *Pfu* DNA polymerase (Stratagene, USA) in standard conditions and the corresponding pTeasy plasmid as template DNA. The purified reaction products of ~550 bp were digested with NcoI and HindIII for 2 h at 37 °C and cloned into the pBAT-4 expression vector (Peränen et al., 1996). The resulting plasmid was named pFRAC and its inserted fragment was verified by DNA sequence analysis.

Expression of recombinant FraC was carried out in *E. coli* BL21 (DE3) cells transformed by electroporation. Bacterial cells were grown at 37 °C in LB culture containing 0.1 mg/ml ampicillin. Protein expression was induced with 1 mM IPTG and, after 5–6 h, the cells were harvested by centrifugation at 8000 × *g* for 10 min. The cell pellet was then suspended in the minimum volume of 50 mM Tris–HCl, pH 7.5 buffer containing 50 μM phenylmethylsulfonyl fluoride (PMSF), frozen in liquid nitrogen and stored overnight at –80 °C. After thawing, the cells were disrupted by sonication in a Soniprep 150 MSE probe sonicator. The suspension was digested with DNAase (final concentration 0.01 mg/ml) at 25 °C for 30 min and centrifuged (50,000 × *g*, 60 min, 4 °C). The supernatant was applied to a cation-exchange SP-Sepharose column and elution conditions were the same as in the purification of native FraC. The fractions with haemolytic activity were concentrated and applied to a HiPrep 16/60 Sephacryl S-300 HR (GE Healthcare, UK) gel-filtration column equilibrated and eluted with 200 mM NaCl, 50 mM Tris–HCl buffer, pH 7.5. The haemolytic fractions were concentrated and desalted by means of Amicon filters and stored at –26 °C until needed.

2.10. Surface pressure measurements

Surface pressure measurements were carried out by the Wilhelmy plate method using a Micro-Trough-S system from Kibron (Helsinki, Finland) at 25 °C with constant stirring. The aqueous subphase consisted of 1 ml of 200 mM NaCl, 10 mM Hepes, pH 7.5. A lipid mixture containing the adequate proportions of PC and SM dissolved in chloroform/methanol (2:1, v/v), was gently spread over the subphase. The desired initial surface pressure was attained by changing the amount of lipid applied to the air–water interface. After 10 min (to allow for solvent evaporation) the protein was injected through a hole connected to the subphase. The final toxin concentration in the Langmuir trough was 1 μM. The resulting increment in surface pressure was recorded until a stable signal was obtained.

Table 1

Primers used in this work. Target sites for the restriction enzymes are underlined.

Name	Sequence	Restriction site
ol_fra1	5' ATATATCCATGGCTGACGTTGCTGGTCTGTTATCGACGG	NcoI
ol_fra3b	5' ATATATCCATGGTTGCTGTTGCTGGTCTATCAATCCAAGGTGC	NcoI
ol_pTb	5' CTGATTGGATCCCTATTTTTTTTTTTTTTTTTTTTTT	BamHI
ol_FraERBS2	5' ATATATCCATGGCCGATGTTGCAGGTGCAGTGATAGACGGTGC	NcoI
ol_Fra1d	5' TCAACAAGCTTCAAGCCITGGTACAGTGAATTCAGTATGGC	HindIII

2.11. Preparation of large unilamellar vesicles and leakage experiments

Equimolar concentrations of PC and SM were dissolved in chloroform:methanol (2:1, v/v) and evaporated thoroughly. The dry lipid film was resuspended by vortexing in 50 mM NaCl, 10 mM HEPES pH 7.5, containing 25 mM ANTS and 90 mM DPX to yield multilamellar vesicles (MLV). The MLV were frozen in liquid nitrogen and thawed in a water bath at 45 °C (10 cycles). Large unilamellar vesicles (LUV) were prepared by extrusion through polycarbonate filters with a pore diameter of 0.1 µm (Nucleopore, Pleasanton, CA, USA) (Mayer et al., 1986). Non-encapsulated fluorescent probes were separated from the vesicle suspension through a Sephadex G-25 column (Amersham Biosciences, GE Healthcare, UK) eluted with isosmotic 200 mM NaCl, 10 mM HEPES, pH 7.5. Solution osmolarities were checked with an Osmomat 030 instrument (Gonotech, Berlin, Germany). Phospholipid concentration was measured according to Barlett (1959).

2.12. Leakage of encapsulated solutes

The leakage of encapsulated solutes was assayed as described by Ellens et al. (1985). Changes in fluorescence intensity were recorded in a FluoroMax-3 spectrofluorometer (Horiba Jobin Yvon, NJ, USA) with excitation and emission wavelengths set at 355 nM and 510 nM, respectively. Liposome concentration was 0.1 mM and toxin was added at a final lipid to protein molar ratio of 150:1. Complete released of the fluorescent probe was achieved by the addition of Triton X-100 (final concentration = 0.1% w/v). The percentage of leakage was calculated as follows:

$$\%leakage = 100 \times [(F_f - F_0)/(F_{100} - F_0)]$$

where F_f is the fluorescence value measured after addition of the toxin, F_0 is the initial fluorescence of the liposome suspension and F_{100} is the fluorescence value measured after addition of Triton X-100. Measurements were carried out at 25 °C with constant stirring.

2.13. Circular dichroism

Far UV (200–250 nM) CD spectra were recorded in a J-810 spectropolarimeter (Jasco Analítica Spain, Madrid, Spain) equipped with a Jasco PTC-423 temperature controller and previously calibrated with d-10-camphorsulphonic acid. The measurements were carried out at 20 °C using stoppered quartz cuvettes with 2 mm path-length. Native and recombinant FraC were dissolved in 20 mM Tris-HCl, pH 8.0 at a concentration of 0.086 mg/ml. Before measurement, the protein samples were centrifuged for 15 min at 14,000 × g in an Eppendorf microcentrifuge at 4 °C. Each experiment was the average of 20 scans and the corresponding baseline was subtracted. Percentages of protein secondary structure from the CD spectra were calculated with the Spectrum Manager program provided by the manufacturer. Thermal denaturation was monitored at 210 nM in 2 mm path-length cuvettes in the temperature range 10–90 °C with a heating

rate of 60 °C h⁻¹. Melting temperatures (T_m) were calculated as the maxima of the first derivatives of the percentage of change of ellipticity at 210 nM vs. temperature curves.

2.14. Multiple sequence alignment

Using FraC as query sequence, BLASTP (<http://blast.ncbi.nlm.nih.gov/Blast.cgi>) (Altschul et al., 1997) was used to retrieve similar sequences from the non-redundant (nr) protein database. CLUSTALW2 (<http://www.ebi.ac.uk/Tools/clustalw2/index.html>) (Higgins et al., 1994) was used to align the actinoporin sequences and the alignment was edited with Jalview (version 2.4) (<http://www.jalview.org/index.html>) (Clamp et al., 2004). In order to highlight the different residues according to the degree of conservation and generate a figure suitable for publication we used Boxshade (version 3.21) (http://www.ch.embnet.org/software/BOX_form.html).

3. Results

3.1. Purification of the native toxins

Fig. 1A shows the elution profile obtained after passing the venom from *A. fragacea* through the cation-exchange chromatography column. Three out of the five peaks obtained were able to permeabilize the erythrocytes, and are labelled in the figure as peaks I, II and III, respectively. The haemolytic activities of the three peaks were different (data not shown).

Fractions associated to each peak were analyzed by SDS-PAGE and the results are shown in Fig. 1B. The first non-haemolytic peak (lane D) contains one band of approximately 18.1 kDa, whereas the second non-haemolytic peak (lane C) contains two bands of approximately 15.0 kDa and 16.3 kDa. Lanes E, F and G (corresponding to haemolytic peaks I, II and III, respectively) yielded a band at approximately 20 kDa, which is the expected value for actinoporins (Maček et al., 1982; Maček and Lebez, 1988; Kem and Dunn, 1988; Khoo et al., 1993; Lanio et al., 2001). In addition to this band, the peak I contained another protein with a slightly lower molecular weight (Fig. 1B, lane E). The silver staining also revealed some minor bands at high molecular weight that could be assigned to the small amount of precipitated material (most likely protein aggregates) that appeared in the chromatographic fractions.

Table 2 shows the N-terminal amino acid sequences (15 residues long) obtained by Edman degradation (Edman and Begg, 1967) of the ~20 kDa bands extracted from the SDS-PAGE gel. Whereas the band obtained from peak II gave rise to one single sequence, peaks I and III contained two different isoforms. Most likely, this is the reason why peaks I and III present a shoulder in the chromatogram (Fig. 1A). Thus, at least five different toxins were revealed by chromatographic separation. The presence of five different toxin isoforms was further confirmed by ion-exchange chromatography using a Mono S[®] HR 5/5 column with superior resolution capacity (data not shown).

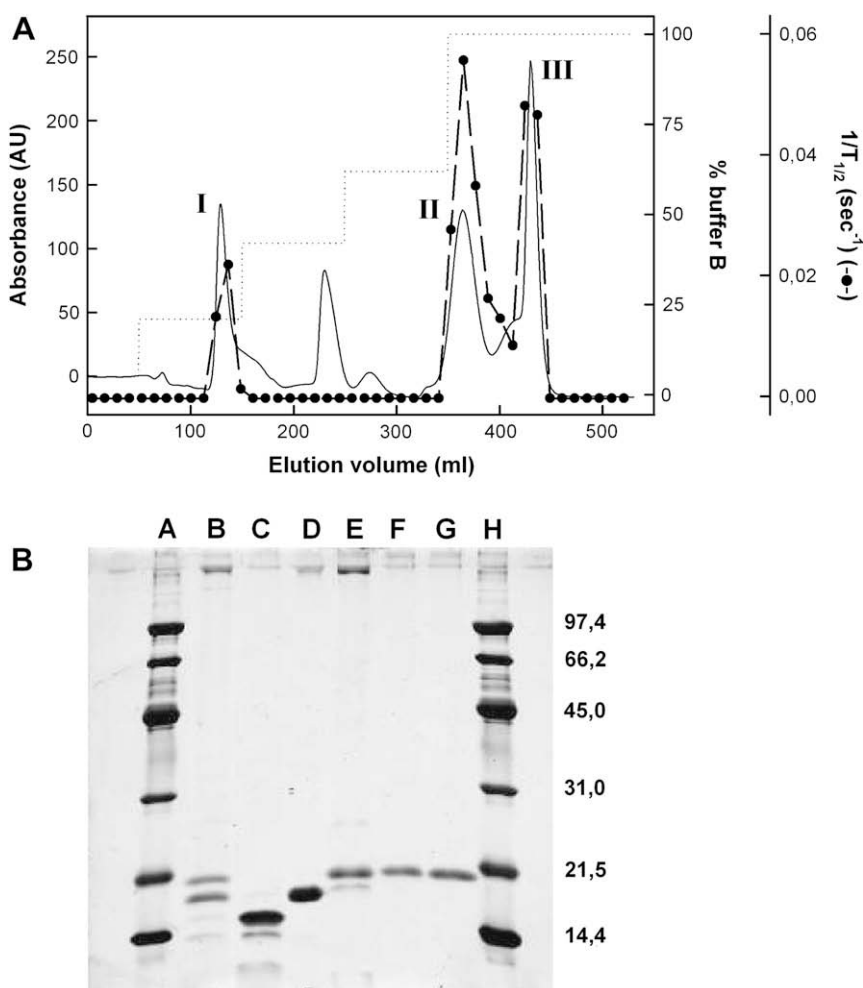


Fig. 1. (A) Chromatogram obtained after passing the venom of *Actinia fragacea* through a SP-sepharose ion-exchange chromatography column. The solid line represents the A_{280} , the dotted line the ionic strength expressed as the proportion of buffer B in the elution buffer and the dashed line with black circles represents the haemolytic activity. (B) Silver stained SDS-PAGE gel of the different chromatographic fractions. Lanes A and H contain the molecular weight markers. Lane B corresponds to the initial venom extract. Lanes D and C were loaded with the first and second peaks without haemolytic activity, respectively. Lanes E, F and G correspond to haemolytic peaks I, II and III, respectively.

3.2. Cloning and determination of the complete amino acid sequence

The RNA isolated from a single specimen of *Actinia fragacea* was used as template for RT-PCR. The cDNA band with a size of ~750 base pairs (Supplementary data) was selected for cloning in a pGEM[®]-T Easy Vector (Clark, 1988) and the ligation mixture was used to transform the *E. coli* XL1-Blue strain. After having some selected clones sequenced, four of the sequences could correspond to actinoporins. These sequences were very similar (data not shown) and we could not tell whether they were actually different protein isoforms, as in other actinoporins (Anderluh et al., 1999; Wang et al., 2008), or the result of mutations introduced by the DNA polymerase itself. Since one of the coding sequences (Fig. 2) partially overlapped with the N-terminal sequence experimentally determined for the toxin eluted in peak II (Table 2) we carried out a proteomic analysis (i.e. molecular mass determination

Table 2

N-terminal sequences corresponding to the proteins obtained from the ~20 kDa SDS-PAGE bands of the haemolytic peaks in Fig. 1A.

Haemolytic peak	N-terminal sequence
Peak I	SAEVA GAVIE GAKLT ----- --I-D --S--
Peak II	SADVA GAVID GAGLG
Peak III	SADVA GAVID GAGLT -VA-- ----K --A-G

Peaks I and III showed heterogeneity in their amino acid composition. The minor component of the mixture is shown in the lower line (only the different amino acids are specified).

		<u>S A D V A G A V I D G A</u>	12
		<u>G L G F D V L K T V L E A L G N V K R K</u>	32
1	AGGTCCTGGGCTTCGACGCTCTGAAAACCGTGTCTCGAAGCACTCGGCAATGTCAAACGAAAG		
		<u>I A V G I D N E S G K T W T A M N T Y F</u>	52
62	ATTGCCGTCGGTATCGACAACGAGTCGGGCAAGACGTGGACCGCAATGAACACATACTTC		
		<u>R S G T S D I V L P H K V A H G K A L L</u>	72
122	CGTTCTGGTACCTCTGATATCGTCCTTCCCCATAAAGTTGCACATGGTAAGGCACTGTCT		
		<u>Y N G Q K N R G P V A T G V V G V I A Y</u>	92
182	TACAACGGTCAGAAAAACGTTGGTCCAGTTGCGACTGGCGTGGTTGGAGTAATGGCTTAT		
		<u>S M S D G N T L A V L F S V P Y D Y N W</u>	112
242	TCCATGAGCGATGGAACACCCCTGGCCGTTTTGTTTCAGCGTTCCTATGACTATAACTGG		
		<u>Y S N W W N V R V Y K G Q K R A D Q R M</u>	132
302	TACAGCAACTGGTGAATGTTAGGGTCTATAAAGGACAAAACGAGCAGACCAGAGGATG		
		<u>Y E E L Y Y H R S P F R G D N G W H S R</u>	152
362	TACGAGGAACCTACTACCATCGGTCTCCATTTTCGAGGGGACATGGCTGGCACTCCAGG		
		<u>G L G Y G L K S R G F M N S S G H A I L</u>	172
422	GGTCTTGATATGGATTGAAGAGCCGTGGATTTCATGAACAGCTCTGGACATGCCATACTG		
		<u>E I H V T K A *</u>	179
482	GAAATTACGTCGACCAAAGCTTAAGATCTTGTGAAAACAAATCAATTGAAATGCTTCCC		
	<i>HindIII</i>		
542	CGAGAAAACCTGATGTAAGACTAGCTAAAAGACTCTAATTTTACCCTGTAAGACAAAAAAA		
602	CTAGATCTTCCCATAACATAAAGACAAATAAAATGAAGCACCAAAAAAAAAAAAAAAAAAAAA		
662	AAAAAATAGGGATCCAATCAG		
	<i>BamHI</i>		

Fig. 2. Partial cDNA coding sequence for fragaceatoxin C (GenBank accession number FM958450). The ORF starts with the second base and the restriction sites are underlined. The corresponding amino acid sequence (Uniprot Knowledgebase accession number P86212) is shown in boldface, where the first twelve amino acids are encoded by the primer oL_FraERBS2. The tryptic fragments identified after proteomic analysis of native FraC (Supplementary information) are underlined.

and identification of tryptic fragments) of this particular toxin (Supplementary data).

Fig. 2 also shows the amino acid sequence coded by the selected plasmid, where the tryptic fragments obtained from the native toxin are underlined. Its estimated *pI* is 9.58, and 164 out of the 179 amino acids (91.6%) have been identified in the tryptic fragments, thus providing good evidence that the cDNA sequence cloned in the plasmid corresponds to the gene coding for the protein present in peak II (Fig. 1A). Furthermore, whereas the theoretical mass for the protein coded by the plasmid is 19,719.25 Da, the actual value obtained by ESI-TOF mass spectrometry of the protein band extracted from the SDS-PAGE gel was $19,719 \pm 3$ Da. Consequently, the plasmid coding for this sequence was named pTeasy-FRA1–3, the DNA coding sequence was named *fraC* and its expression product FraC. The actinoporin cDNA sequence obtained in this way is only partial since the first 32 coding nucleotides belong to the forward primer used for cDNA amplification. The cDNA sequence extracted from *Actinia fragacea* has been deposited in the EMBL nucleotide database (accession number FM958450) and the protein sequence data reported in this paper will appear in the UniProt Knowledgebase under the accession number P86212.

3.3. Sequence analysis

After running BLASTP (NCBI server) using FraC as query sequence and the nr database, it became apparent that FraC contains the conserved domain characteristic of the anemone_cytotox protein family (Pfam code PF06369). Fourteen different proteins were found with

more than 55% sequence identity (76% sequence similarity). These 15 proteins were loaded into CLUSTALW2 (EMBL-EBI server) for multiple sequence alignment and the result is shown in Fig. 3. FraC conserves the tryptophan-rich region containing Trp-112 and Trp-116, which are crucial for membrane binding (Hong et al., 2002), and Trp-117, which confers stability to the protein (Kristan et al., 2004). The amino acid residues that participate in the phosphorylcholine binding pocket (Val-87, Pro-107, Ser-54, Ser-105, Tyr-113, Tyr-133, Tyr-137 and Tyr-138) (Mancheño et al., 2003) are also conserved, suggesting that its mechanism of action be identical to that of equinatoxin-II and sticholysin-II. As in the rest of actinoporins, the N and C termini are the less conserved regions. Multiple sequence alignment was also performed with Toffee and EXPRESSO (<http://tcoffee.org>). The latter program utilizes the sequences and all the available structural information in the Protein Data Bank to produce the best possible alignment. Both programs yielded essentially the same result (data not shown).

3.4. Expression and purification of recombinant fragaceatoxin C

The cDNA sequence coding for FraC was amplified by PCR (Peränen et al., 1996). The forward primer (oL_FraERBS2) codes for the experimentally determined N-terminal sequence of FraC. It carries the mutation S1M to allow for expression in *E. coli* and was designed to minimize the formation of mRNA secondary structures that could interfere with translation (Hofacker, 2003; Alegre-Cebollada et al., 2007b). The reverse primer (oL_Fra1d) carries a mutation in the DNA sequence that eliminates a HindIII restriction site near the 3' end of the FraC open reading

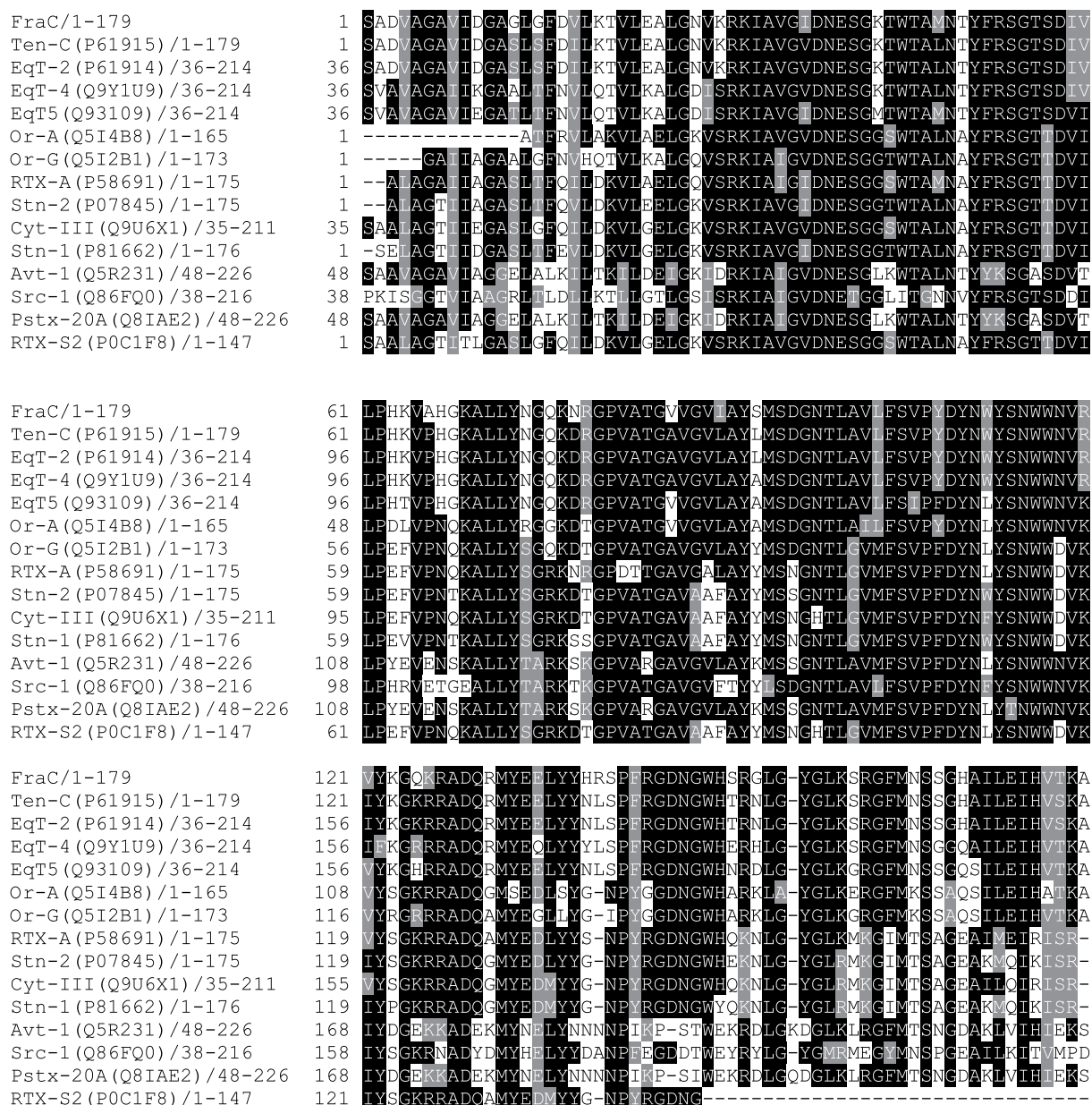


Fig. 3. Multiple sequence alignment of actinoporins. The numbering corresponds to the original sequences as stored in the Uniprot Knowledgebase. The alignment was built with CLUSTALW2, edited with Jalview and shaded with Boxshade.

frame without changing the amino acid sequence and introduces a new restriction site for HindIII immediately after the stop codon (Fig. 2). The amplified sequence was then cloned into the expression vector pBAT-4.

The purification of recombinant FraC required two chromatographic steps. The bacterial crude extract was first applied to an ion-exchange chromatography column and the single haemolytic peak only eluted when the proportion of buffer B in the eluent mixture reached 100% (Fig. 4A). Then, the fractions with haemolytic activity were subjected to gel-filtration chromatography (Fig. 4B). Interestingly, the recombinant FraC only eluted after passing 3

void-volumes of buffer through the gel-filtration column, most likely due to some specific interaction with the resin. After purification, the toxin yield was 0.5 mg of recombinant FraC per liter of bacterial culture.

Recombinant FraC was purified to homogeneity and its electrophoretic mobility within the gel was identical to that of native FraC (Fig. 4B, inset). Whereas the theoretical mass for the recombinant protein (considering the S1M mutation) is 19,763.4 Da, the molecular mass obtained by ESI-TOF Mass spectrometry was only 19,632.5 (Supplementary data). This difference could be explained by the processing of *E. coli* proteins by

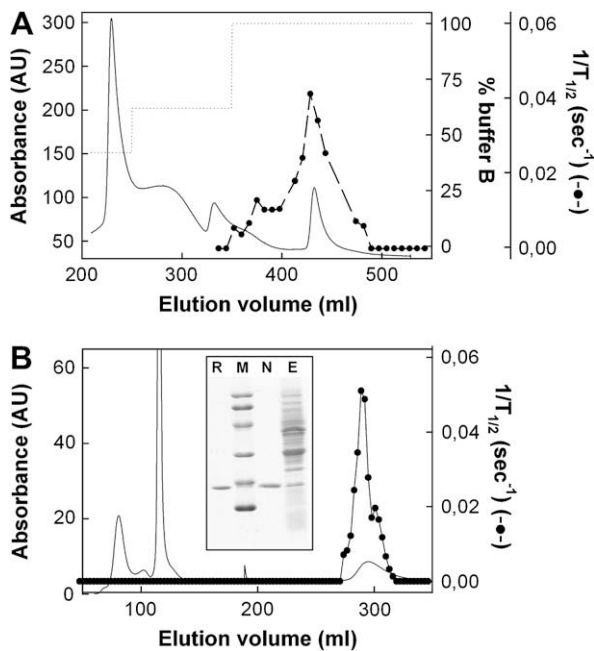


Fig. 4. Purification of recombinant FraC. (A) Ion-exchange chromatography. The solid line represents the A_{280} , the dotted line the ionic strength expressed as the proportion of buffer B in the elution buffer and the dashed line with black circles represents the haemolytic activity. (B) Gel-filtration chromatography. The solid line represents the A_{280} and the dashed line with black circles represents the haemolytic activity. Inset: Coomassie-stained SDS-PAGE gel of the initial bacterial crude extract (lane E), native FraC (lane N), recombinant FraC (lane R) and the molecular weight markers (lane M).

methionine aminopeptidase, an enzyme that catalyzes the removal of amino-terminal methionine from proteins (Ben-Bassat et al., 1987).

3.5. Haemolytic activity of native and recombinant FraC

The haemolytic activities of native and recombinant FraC are shown in Fig. 5. For both proteins there is a threshold concentration value (~ 0.8 nM) below which there is no haemolysis in the time scale of the experiment.

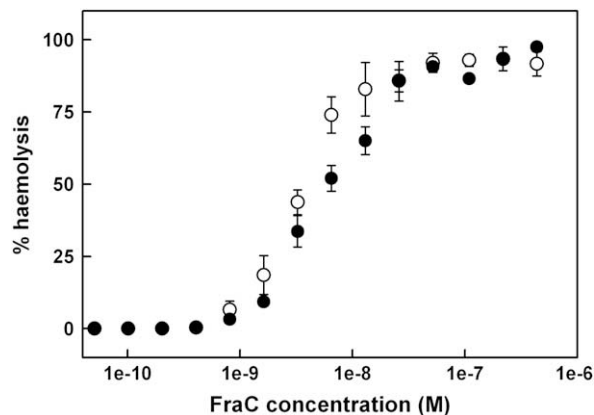


Fig. 5. Concentration dependence of the haemolytic activity of native (○) and recombinant FraC (●).

On the other hand, at concentrations above 50 nM both toxins are practically 100% haemolytic. Within this concentration range haemolysis is partial and native FraC seems to be slightly more active than recombinant FraC. The concentration that lyses 50% of the erythrocytes is ~ 4 nM for native FraC and ~ 6.5 nM for recombinant FraC.

3.6. Surface pressure measurements

Fig. 6A shows the kinetic traces of insertion of native and recombinant FraC into monolayers made of PC/SM (1/1). We chose this lipid composition because all the actinoporins studied so far exhibit maximum activity in these conditions (Tejuca et al., 1996; De los Ríos et al., 1998; Caaveiro et al., 2001; Barlič et al., 2004). The initial surface pressure (π) was 20 mN/m and the injection of both toxins into the subphase (final concentration of 1 μ M) resulted in an increase in the surface pressure of approximately 12 mN/m.

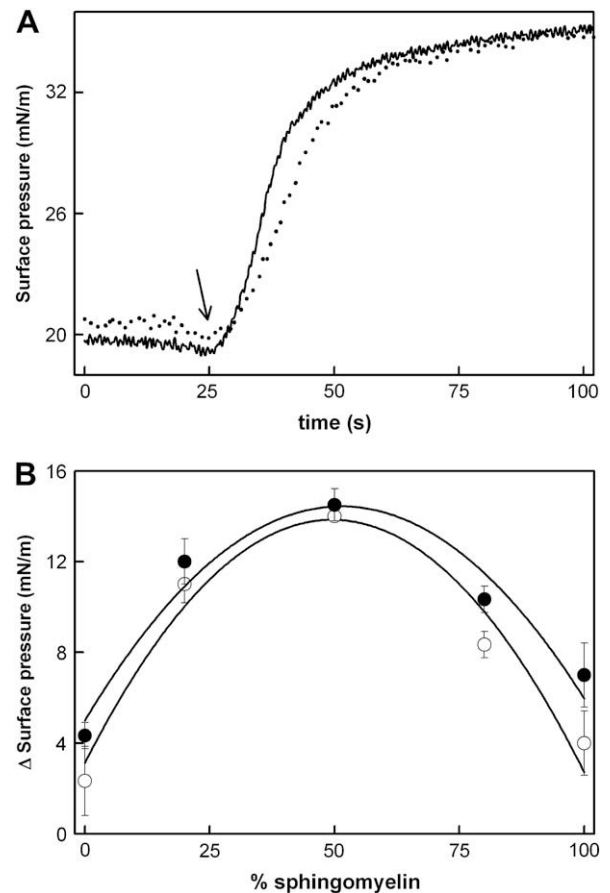


Fig. 6. (A) Penetration of native (solid line) and recombinant FraC (dotted line) into a lipid monolayer made of SM/PC (1:1). The arrow indicates the addition of the toxin (final concentration in the subphase = 1 μ M). (B) Increase in the surface pressure after insertion of native (○) and recombinant FraC (●) into lipid monolayers made of different mixtures of PC and SM. Experimental data are fitted to a polynomial function (degree = 2). Symbols correspond to the mean \pm standard deviations of two or three independent measurements.

Next, we changed the PC/SM proportion in the lipid mixture to determine if native and recombinant FraC responded in the same way to changes in lipid composition. The results are shown in Fig. 6B. Both toxins exhibit maximum penetration at equimolar PC/SM mixtures, as already observed with sticholysins (Tejuca et al., 1996; De los Ríos et al., 1998) and equinatoxin-II (Caaveiro et al., 2001; Barlič et al., 2004). The increase in the surface pressure is significantly smaller when the mixture is enriched in either lipid.

3.7. Critical pressure and liposome permeabilization

The critical pressure can be defined as the initial surface pressure of a lipid monolayer at which no protein penetration occurs and this parameter is related to its ability to penetrate a membrane with a given lipid composition. There is a linear relationship between the initial surface pressure of the monolayer and the increase in surface pressure that takes place after injection of the toxin into the subphase. Extrapolation of this straight line to the abscissa axis yields the critical pressure. Critical pressures for native and recombinant FraC are 36.3 mN/m and 37.6 mN/m, respectively (Fig. 7A). This result indicates that both proteins could permeabilize membranes, since the estimated surface pressure of the membrane bilayer is ~ 31 mN/m (Demel et al., 1975). In fact, the addition of native or recombinant FraC to liposomes made of SM/PC (1:1) resulted in the immediate release of 87% of the encapsulated solute (Fig. 7B).

3.8. Circular dichroism and thermal stability

Fig. 8A shows differential circular dichroism spectra for both, native and recombinant FraC, in the far UV region. Both proteins have similar spectra, with a low-intensity negative band at 217 nM, characteristic of proteins with high content in β -sheet secondary structure (Greenfield and Fasman, 1969). From these spectra, the built-in software calculated 13.4% α -helix and 56.5% β -sheet for native FraC and 16.2% α -helix and 51.4% β -sheet for recombinant FraC. Although these figures must be considered with some caution, they are in good agreement with the 12% α -helix and 46% β -sheet for equinatoxin-II (data obtained from the 1iaz registry in the Protein Data Bank) and 12% α -helix and 48% β -sheet for sticholysin-II (data obtained from the 1gw registry in the Protein Data Bank).

The thermal denaturation profiles of native and recombinant FraC were obtained by monitoring the variation in the ellipticity at 210 nM in the temperature range between 10 °C and 90 °C and are shown in Fig. 8B. Both profiles are superimposable, with half-transition temperatures (T_m) of 55.8 °C (native FraC) and 56.2 °C (recombinant FraC).

4. Discussion

The purification protocol for actinoporins from *Actinia fragacea* is largely based on the isolation of recombinant equinatoxin-II (Anderluh et al., 1996), which avoids the acetone precipitation step described for the purification of native equinatoxin-II (Maček et al., 1988). We considered

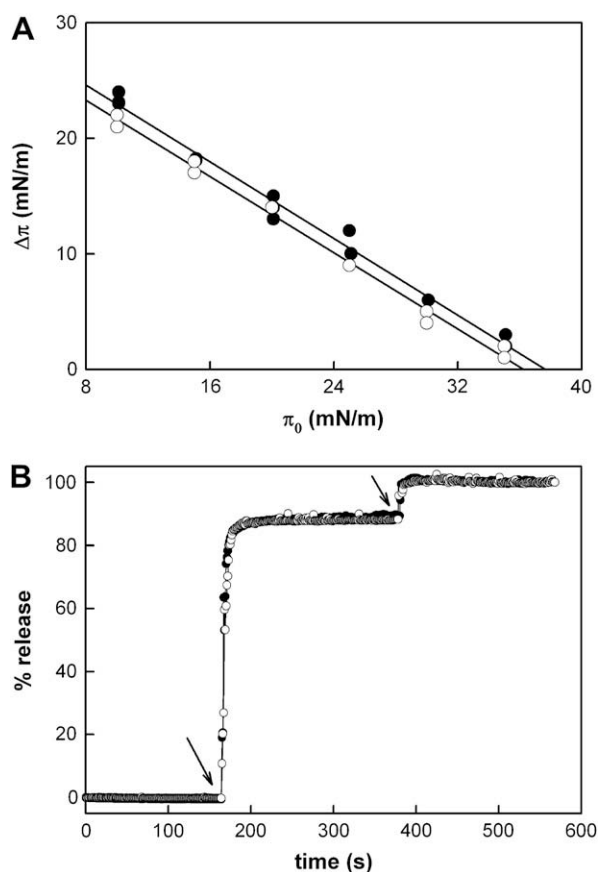


Fig. 7. (A) Critical pressures of native and recombinant FraC in a lipid monolayer made of SM/PC (1:1). (○) Native FraC. (●) Recombinant FraC. (B) Percentage of release of fluorescent solutes encapsulated in LUV made of SM/PC (1:1) by native (○) and recombinant FraC (●). The first arrow indicates the addition of the toxin and the second the addition of Triton X-100 at a final concentration of 0.1% (w/v).

the selective precipitation of proteins unnecessary because the haemolytic toxins were the major components of the anemone venom and we preferred to maintain them in their native conformation. In addition, we minimized the protein loss, which inevitably takes place after acetone precipitation, thus increasing the chance of detecting other minor components of the venom. The chromatogram obtained after passing the venom of *A. fragacea* through a cation-exchange resin yielded three haemolytic peaks (Fig. 1A). The haemolytic activity was associated to the ~ 20 kDa band (Fig. 1B) and was different for each peak.

N-terminal sequencing revealed the existence of, at least, five isoforms, since peaks I and III contained ambiguities in protein sequence (Table 2). The presence of different toxin isoforms with slightly different sequences and different haemolytic activities is a recurring theme in actinoporins. To name but a few examples, five isoforms from *A. equina* have been described so far (and more may exist) (Anderluh et al., 1999), three isoforms were isolated from *A. cari* (Maček et al., 1982), three from *A. tenebrosa* (Norton et al., 1990), four from *Stichodactyla helianthus* (Kem and Dunn, 1988), two from *Oulactis orientalis* (Il'ina

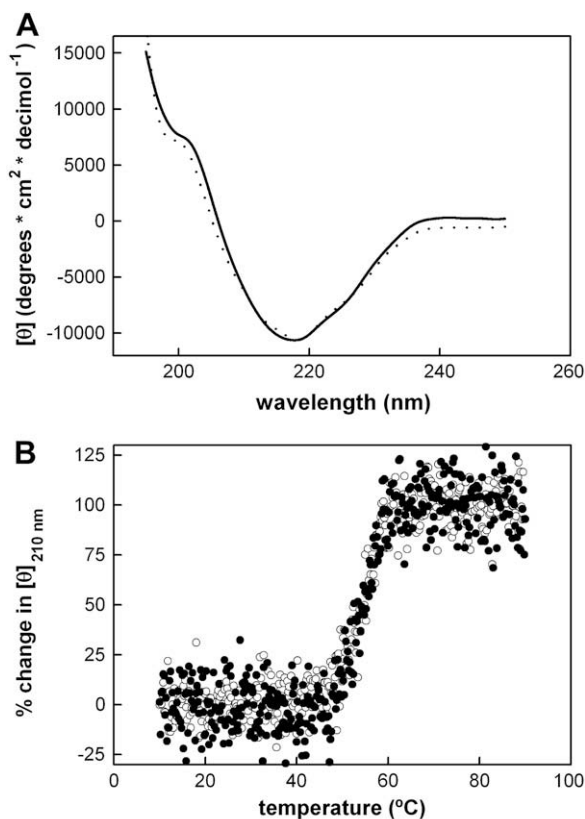


Fig. 8. (A) Far UV-CD spectra of native (solid line) and recombinant FraC (dotted line). In each case, the baselines have been subtracted. (B) Thermal stability of native (○) and recombinant FraC (●) as monitored by changes in ellipticity at 210 nm. Data are expressed as percentage of total change.

et al., 2005) and, at the genomic level, more than 50 different gene sequences have been cloned from *Heteractis magnifica* (Wang et al., 2008). Thus, fragaceatoxins may also belong to a multigene family, which could have arisen by gene duplication and subsequent gene conversion or mutation (Anderluh et al., 1995; Wang et al., 2008). Hence, the different actinoporin isoforms are not allelic variants but paralogs.

From the cDNA obtained after RT-PCR of the RNA extracted from a single specimen of *A. fragacea* we obtained a coding sequence whose expression product partially overlapped with the N-terminal sequence determined by Edman degradation of the actinoporin present in peak II (Table 2), which we named FraC. Thus, within the expression vector, the N-terminal amino acid sequence of FraC (residues 1–12) is coded by the oL_FraERBS2 primer whereas the rest of the protein (from Gly-13 to the C terminus) is coded by the cDNA sequence obtained from the natural source (Fig. 2). The proteomic analysis (i.e. identification of the tryptic fragments and estimation of the molecular mass) revealed that the cloned sequence corresponded to that of the native protein. This result indicates that the protein does not undergo any post-translational modifications.

The multiple sequence alignment of actinoporins indicates that the N-terminal regions show great variation.

Since this region is essential for the formation of a functional pore (Hong et al., 2002; Malovrh et al., 2003; Kristan et al., 2004), this variability could account for the differences in haemolytic activity observed among the diverse isoforms of these and other sea anemone toxins, their N-truncated mutants or their N-terminal synthetic peptides (Anderluh et al., 1997; Huerta et al., 2001; Casalanovo et al., 2006; Cilli et al., 2007). The C-terminal regions also exhibit great variability, although the exact role played by this region in pore formation is far from being understood. Conversely, the central part of the protein is largely conserved. This region contains the characteristic β -sandwich motif of actinoporins (Athanasiadis et al., 2001), which is involved in the specific lipid binding that takes place prior to N-terminal helix insertion and pore formation (Hong et al., 2002). The specificity of the binding is brought about by the exposed tryptophan-rich region containing Trp-112 and Trp-116 (Malovrh et al., 2000; Hong et al., 2002; Bakrač et al., 2008) and by the conserved phosphorylcholine binding pocket observed in sticholysin-II (Mancheño et al., 2003). Although the membrane attachment of this β -sandwich is shallow, it may provide a rigid scaffold that helps to stabilize the final transmembrane pore (Anderluh and Lakey, 2008).

4.1. Native vs. recombinant FraC

Recombinant FraC was expressed in *E. coli* and purified by ion-exchange and gel-filtration chromatography. Circular dichroism spectra of native and recombinant FraC are practically identical and show that they are mainly beta proteins, a hallmark of actinoporins (Belmonte et al., 1994; Mancheño et al., 2001). The thermal stability of both proteins is identical, with denaturation midpoints centered at 55.8 °C (native FraC) and 56.2 °C (recombinant FraC). These values are significantly lower than the 65 °C reported for equinatoxin-II and sticholysin-II (Poklar et al., 1997; Mancheño et al., 2001; Kristan et al., 2004). This result indicates that FraC might interact more readily with cell or model membranes than other actinoporins.

The haemolytic activity is strongly dependent on the type of erythrocytes used (Maček et al., 1994 and references within), their age (Celedón et al., 2008) and the particular actinoporin under study and, therefore, is very often used for comparative purposes (Huerta et al., 2001; Cilli et al., 2007). The haemolytic activities of native and recombinant FraC are very similar. They start to lyse sheep erythrocytes at a concentration of 0.8 nM and above 50 nM haemolysis is complete. The small differences observed within this concentration range can be explained by the processing of the N-terminal amino acid residue that takes place during the expression of recombinant FraC in *E. coli* (Ben-Bassat et al., 1987). Cilli et al. (2007) have shown that in peptides containing the first 30 amino acids of sticholysin-I, the absence of one single amino acid at the N-terminus slightly modifies its haemolytic activity.

The insertion of native and recombinant FraC into lipid monolayers depends strongly on their SM content (Fig. 6B). This result suggests a preferential binding of actinoporins to the interfaces between lipid phases and this behaviour seems to be common to actinoporins either in cell or model

membranes (Tejuca et al., 1996; Barlič et al., 2004; Alegre-Cebollada et al., 2006; Bakrač et al., 2008). Within the lipid bilayer, the surface pressure is approximately 31 mN/m (Demel et al., 1975) and only peptides or proteins capable of penetrating a monolayer at 31 mN/m or more would permeabilize cell or model membranes. Both, native and recombinant FraC have critical pressures well above this threshold value and, therefore, will permeabilize PC/SM (1:1) bilayers. This conclusion was confirmed by the release of fluorescent solutes encapsulated in LUVs (Fig. 7B). Moreover, in Fig. 7A the regression lines have the same negative slope, an indication that the degree of membrane penetration of both proteins is identical (Hong et al., 2002).

In conclusion, from the venom of *Actinia fragacea* five different actinoporins have been identified by ion-exchange column chromatography. One of them (FraC) has been cloned and expressed in *E. coli*. Native and recombinant FraC are structurally and functionally identical and their interaction with model and lipid membranes share the same basic features already described for equinatoxin-II and sticholysin-II. Multiple sequence analysis indicates that FraC belongs to the anemone_cytotox protein family as, most likely, the remaining four isotoxins. However, this result awaits further investigation and will be the subject of a forthcoming publication.

Acknowledgments

A. B. is a staff scientist from the CONICET and the recipient of a postdoctoral fellowship from the Basque Government. K. M. is the recipient of a predoctoral fellowship from the Spanish Ministerio de Educación y Ciencia. This work was supported in part by Grant BFU 2007-62062 (Ministerio de Educación y Ciencia) and Grant IT 461-07 (University of the Basque Country). Mass spectrometry analysis was performed in the Proteomics Unit (member of ProteoRed) at the University of the Basque Country by Kerman Aloria.

Conflict of interest

There are no conflicts of interest.

Appendix. supplementary material

The agarose gel showing the PCR products obtained from the cDNA of *Actinia fragacea* and the proteomic methods and results are included as supplementary information.

Supplementary data associated with this article can be found in the online version, at [10.1016/j.toxicon.2009.06.022](https://doi.org/10.1016/j.toxicon.2009.06.022).

References

- Alegre-Cebollada, J., Rodríguez-Crespo, I., Gavilanes, J.G., Martínez del Pozo, A., 2006. Detergent-resistant membranes are platforms for actinoporin pore-forming activity on intact cells. *FEBS J* 273, 863–871.
- Alegre-Cebollada, J., Oñaderra, M., Gavilanes, J.G., Martínez del Pozo, A., 2007a. Sea anemone actinoporins: the transition from a folded soluble state to a functionally active membrane-bound oligomeric pore. *Curr. Protein Pept. Sci.* 8, 558–572.
- Alegre-Cebollada, J., Clementi, G., Cuniatti, M., Porres, C., Oñaderra, M., Gavilanes, J.G., Martínez del Pozo, A., 2007b. Silent mutations at the 5'-end of the cDNA of actinoporins from the sea anemone *Stichodactyla helianthus* allow their heterologous overproduction in *Escherichia coli*. *J. Biotechnol* 127, 211–221.
- Altschul, S.F., Madden, T.L., Schäffer, A.A., Zhang, Z., Miller, W., Lipman, D.J., 1997. Gapped BLAST and PSI-BLAST: a new generation of protein database search programs. *Nucleic Acids Res.* 25, 3389–3402.
- Álvarez, C., Mancheño, J.M., Martínez, D., Tejuca, M., Pazos, F., Lanio, M.E., 2009. Sticholysins, two pore-forming toxins produced by the Caribbean Sea anemone *Stichodactyla helianthus*: their interaction with membranes. *Toxicon*. doi:10.1016/j.toxicon.2009.02.022.
- Anderluh, G., Lakey, J.H., 2008. Disparate proteins use similar architectures to damage membranes. *Trends Biochem. Sci.* 33, 482–490.
- Anderluh, G., Maček, P., 2002. Cytolytic peptide and protein toxins from sea anemones (Anthozoa: Actiniaria). *Toxicon* 40, 111–124.
- Anderluh, G., Štrukelj, B., Maček, P., Gubenšek, F., 1995. The coding region of the equinatoxin II gene lacks introns. *Croat. Chem. Acta* 68, 533–542.
- Anderluh, G., Pungerčar, J., Štrukelj, B., Maček, P., Gubenšek, F., 1996. Cloning, sequencing and expression of equinatoxin II. *Biochem. Biophys. Res. Commun.* 220, 437–442.
- Anderluh, G., Pungerčar, J., Križaj, I., Štrukelj, B., Gubenšek, F., Maček, P., 1997. N-terminal truncation mutagenesis of equinatoxin II, a pore-forming protein from the sea anemone *Actinia equina*. *Protein Eng* 10, 751–755.
- Anderluh, G., Križaj, I., Štrukelj, B., Gubenšek, F., Maček, P., Pungerčar, J., 1999. Equinatoxins, pore-forming proteins from the sea anemone *Actinia equina*, belong to a multigene family. *Toxicon* 37, 1391–1401.
- Athanasiasidis, A., Anderluh, G., Maček, P., Turk, D., 2001. Crystal structure of the soluble form of equinatoxin II, a pore-forming toxin from the sea anemone *Actinia equina*. *Structure* 9, 341–346.
- Bakrač, B., Gutiérrez-Aguirre, I., Podlesek, Z., Sonnen, A.F., Gilbert, R.J., Maček, P., Lakey, J.H., Anderluh, G., 2008. Molecular determinants of sphingomyelin specificity of a eukaryotic pore-forming toxin. *J. Biol. Chem.* 283, 18665–18677.
- Barlett, G.R., 1959. Phosphorus assay in column chromatography. *J. Biol. Chem.* 334, 466–468.
- Barlič, A., Gutiérrez-Aguirre, I., Caaveiro, J.M.M., Cruz, A., Ruiz-Argüello, M. B., Pérez-Gil, J., González-Mañás, J.M., 2004. Lipid phase coexistence favors membrane insertion of equinatoxin-II, a pore-forming toxin from *Actinia equina*. *J. Biol. Chem.* 279, 34209–34216.
- Belmonte, G., Menestrina, G., Pederzoli, C., Križaj, I., Gubenšek, F., Turk, T., Maček, P., 1994. Primary and secondary structure of a pore-forming toxin from the sea anemone, *Actinia equina* L., and its association with lipid vesicles. *Biochim. Biophys. Acta* 1192, 197–204.
- Ben-Bassat, A., Bauer, K., Chang, S.Y., Myambo, K., Boosman, A., Chang, S., 1987. Processing of the initiation methionine from proteins: properties of the *Escherichia coli* methionine aminopeptidase and its gene structure. *J. Bacteriol* 169, 751–757.
- Caaveiro, J.M., Echabe, I., Gutiérrez-Aguirre, I., Nieva, J.L., Arrondo, J.L.R., González-Mañás, J.M., 2001. Differential interaction of equinatoxin II with model membranes in response to lipid composition. *Biophys. J.* 80, 1343–1353.
- Carter, M.A., Thorpe, J.P., 1981. Reproductive, genetic and ecological evidence that *Actinia equina* var. *mesembryanthemum* and var. *fragacea* are not conspecific. *J. Mar. Biol. Assoc. UK* 61, 71–93.
- Casallanovo, F., de Oliveira, F.J.F., de Souza, F.C., Ros, U., Martínez, Y., Pentón, D., Tejuca, M., Martínez, D., Pazos, F., Pertinhez, T.A., Spisni, A., Cilli, E.M., Lanio, M.E., Alvarez, C., Schreier, S., 2006. Model peptides mimic the structure and function of the N-terminus of the pore-forming toxin sticholysin II. *Biopolymers* 84, 169–180.
- Celedón, G., González, G., Barrientos, D., Pino, J., Venegas, F., Lissi, E.A., Soto, C., Martínez, D., Álvarez, C., Lanio, M.E., 2008. Sticholysin II, a cytolytic toxin from the sea anemone *Stichodactyla helianthus* promotes higher hemolysis in aged red blood cells. *Toxicon* 51, 1383–1390.
- Chomczynski, P., Sacchi, N., 1987. Single-step method of RNA isolation by acid guanidinium thiocyanate-phenol-chloroform extraction. *Anal. Biochem* 162, 156–159.
- Cilli, E.M., Pigossi, F.T., Crusca Jr., E., Ros, U., Martínez, D., Lanio, M.E., Alvarez, C., Schreier, S., 2007. Correlations between differences in amino-terminal sequences and different hemolytic activity in sticholysins. *Toxicon* 50, 1201–1204.
- Clamp, M., Cuff, J., Searle, S.M., Barton, G.J., 2004. The Jalview Java alignment editor. *Bioinformatics* 20, 426–427.
- Clark, J.M., 1988. Novel non-templated nucleotide addition reactions catalyzed by procaryotic and eucaryotic DNA polymerases. *Nucleic Acids Res.* 16, 9677–9686.
- De los Ríos, V., Mancheño, J.M., Lanio, M.E., Oñaderra, M., Gavilanes, J.G., 1998. Mechanism of the leakage induced on lipid model membranes

- by the hemolytic protein sticholysin II from the sea anemone *Stichodactyla helianthus*. *Eur. J. Biochem* 252, 284–289.
- Demel, R.A., Geurts van Kessel, W.S.M., Zwaal, R.F.A., Roelofsens, B., van Deenen, L.L.M., 1975. Relation between various phospholipase actions on human red cell membranes and the interfacial phospholipid pressure in monolayers. *Biochim. Biophys. Acta* 406, 97–107.
- Edman, P., Begg, G., 1967. A protein sequenator. *Eur. J. Biochem* 1, 80–91.
- Ellens, H., Bentz, J., Szoka, F.C., 1985. H^+ - and Ca^{2+} -induced fusion and destabilization of liposomes. *Biochemistry* 24, 3099–3106.
- Finn, R.D., Tate, J., Mistry, J., Coghill, P.C., Sammut, J.S., Hotz, H.R., Ceric, G., Forslund, K., Eddy, S.R., Sonnhammer, E.L., Bateman, A., 2008. The Pfam protein families database. *Nucleic Acids Res. Database Issue* 36, D281–D288.
- Gill, S.C., von Hippel, P.H., 1989. Calculation of protein extinction coefficients from amino acid sequence data. *Anal. Biochem* 182, 319–326.
- Greenfield, N., Fasman, G.D., 1969. Computed circular dichroism spectra for the evaluation of protein conformation. *Biochemistry* 8, 4108–4116.
- Higgins, D., Thompson, J., Gibson, T., Thompson, J.D., Higgins, D.G., Gibson, T.J., 1994. CLUSTAL W: improving the sensitivity of progressive multiple sequence alignment through sequence weighting, position-specific gap penalties and weight matrix choice. *Nucleic Acids Res.* 22, 4673–4680.
- Hofacker, I.L., 2003. Vienna RNA secondary structure server. *Nucleic Acids Res.* 31, 3429–3431.
- Hong, Q., Gutiérrez-Aguirre, I., Barlič, A., Malovrh, P., Kristan, K., Podlesek, Z., Maček, P., Turk, D., González-Mañas, J.M., Lakey, J.H., Anderlüh, G., 2002. Two-step membrane binding by Equinatoxin II, a pore-forming toxin from the sea anemone, involves an exposed aromatic cluster and a flexible helix. *J. Biol. Chem.* 277, 41916–41924.
- Honma, T., Shiomi, K., 2005. Peptide toxins in sea anemones: structural and functional aspects. *Mar. Biotechnol* 8, 1–10.
- Huerta, V., Morera, V., Guanche, Y., China, G., González, L.J., Betancourt, L., Martínez, D., Alvarez, C., Lanio, M.E., Besada, V., 2001. Primary structure of two cytolysin isoforms from *Stichodactyla helianthus* differing in their hemolytic activity. *Toxicon* 39, 1253–1256.
- Il'ina, A.P., Monastyrnaya, M.M., Sokotun, I.N., Egorov Ts. A., Nazarenko, Y. A., Likhatskaia, G.N., Kozlovskaya, E.P., 2005. Actinoporins from the Sea of Japan anemone *Oulactis orientalis*: isolation and partial characterization. *Russ. J. Bioorg. Chem.* 31, 39–48.
- Kem, W.R., Dunn, B.M., 1988. Separation and characterization of four different amino acid sequence variants of a sea anemone (*Stichodactyla helianthus*) protein cytolysin. *Toxicon* 26, 997–1008.
- Khoo, K.S., Kam, W.K., Khoo, H.E., Gopalakrishnakone, P., Chung, M.C.M., 1993. Purification and partial characterization of two cytolysins from a tropical sea anemone *Heteractis magnifica*. *Toxicon* 31, 1567–1579.
- Kristan, K., Podlesek, Z., Hojnik, V., Gutiérrez-Aguirre, I., Gunčar, G., Turk, D., González-Mañas, J.M., Lakey, J.H., Maček, P., Anderlüh, G., 2004. Pore formation by equinatoxin, a eukaryotic pore-forming toxin, requires a flexible N-terminal region and a stable beta-sandwich. *J. Biol. Chem.* 279, 46509–46517.
- Kristan, K., Viero, G., Dalla Serra, M., Maček, P., Anderlüh, G., 2009. Molecular mechanism of pore formation by actinoporins. *Toxicon*. doi:10.1016/j.toxicon.2009.02.026.
- Laemmli, U.K., 1970. Cleavage of structural proteins during the assembly of the head of bacteriophage T4. *Nature* 227 (259), 680–685.
- Lanio, M.E., Morera, V., Álvarez, C., Tejuca, M., Gómez, T., Pazos, F., Besada, V., Martínez, D., Huerta, V., Padrón, G., Chávez, M.A., 2001. Purification and characterization of two hemolysins from *Stichodactyla helianthus*. *Toxicon* 39, 187–194.
- Louw, A.I., Visser, L., 1977. Kinetics of erythrocyte lysis by snake venom cardiotoxins. *Biochim. Biophys. Acta* 498, 143–153.
- Maček, P., Lebez, D., 1988. Isolation and characterization of three lethal and hemolytic toxins from the sea anemone *Actinia equina* L. *Toxicon* 26, 441–451.
- Maček, P., Senčič, L., Lebez, D., 1982. Isolation and partial characterization of three lethal and hemolytic toxins from the sea anemone *Actinia cari*. *Toxicon* 20, 181–185.
- Maček, P., Belmonte, G., Pederzoli, C., Menestrina, G., 1994. Mechanism of action of equinatoxin II, a cytolysin from the sea anemone *Actinia equina* L. belonging to the family of actinoporins. *Toxicology* 87, 205–227.
- Malovrh, P., Barlič, A., Podlesek, Z., Maček, P., Menestrina, G., Anderlüh, G., 2000. Structure-function studies of tryptophan mutants of equinatoxin II, a sea anemone pore-forming protein. *Biochem. J.* 346, 223–232.
- Malovrh, P., Viero, G., Dalla Serra, M., Podlesek, Z., Lakey, J.H., Maček, P., Menestrina, G., Anderlüh, G., 2003. A novel mechanism of pore formation. Membrane penetration by the N-terminal amphipathic region of equinatoxin II. *J. Biol. Chem.* 278, 22678–22685.
- Mancheño, J.M., De Los Ríos, V., Martínez Del Pozo, A., Lanio, M.E., Oñaderra, M., Gavilanes, J.G., 2001. Partially folded states of the cytolytic protein sticholysin II. *Biochim. Biophys. Acta* 1545, 122–131.
- Mancheño, J.M., Martín-Benito, J., Martínez-Ripoll, M., Gavilanes, J.G., Hermoso, J.A., 2003. Crystal and electron microscopy structures of sticholysin II actinoporin reveal insights into the mechanism of membrane pore formation. *Structure* 11, 1319–1328.
- Mayer, L.D., Hope, M.J., Cullis, P.R., 1986. Vesicles of variable sizes produced by a rapid extrusion procedure. *Biochim. Biophys. Acta* 858, 161–168.
- Norton, R.S., Bobek, G., Ivanov, J.O., Thomson, M., Fiala-Beer, E., Moritz, R.L., Simpson, R.J., 1990. Purification and characterisation of proteins with cardiac stimulatory and haemolytic activity from the anemone *Actinia tenebrosa*. *Toxicon* 28, 29–41.
- Peränen, J., Rikkonen, M., Hyvönen, M., Kääriäinen, L., 1996. T7 vectors with modified T7lac promoter for expression of proteins in *Escherichia coli*. *Anal. Biochem* 236, 371–373.
- Perrin, M.C., Thorpe, J.P., Solé-Cava, A.M., 1999. Population structuring, gene dispersal and reproduction in the *Actinia equina* species group. *Oceanogr. Mar. Biol. Annu. Rev.* 37, 129–152.
- Poklar, N., Lah, J., Salobir, M., Maček, P., Vesnaver, G., 1997. pH and temperature-induced molten globule-like denatured states of equinatoxin II: a study by UV-melting, DSC, far- and near-UV CD spectroscopy, and ANS fluorescence. *Biochemistry* 36, 14345–14352.
- Sambrook, J., Russel, D.W., 2001. *Molecular Cloning: a Laboratory Manual*, third ed. Cold Spring Harbor Laboratory Press, Cold Spring Harbor, NY.
- Tejuca, M., Dalla Serra, M., Ferreras, M., Lanio, M.E., Menestrina, G., 1996. Mechanism of membrane permeabilization by sticholysin I, a cytolysin isolated from the venom of the sea anemone *Stichodactyla helianthus*. *Biochemistry* 26, 14947–14957.
- Walton, C.L., 1911. Notes on various British Anthozoa. *J. Mar. Biol. Assoc. UK* 9, 236–242.
- Wang, Y., Yap, L.L., Chua, K.L., Khoo, H.E., 2008. A multigene family of *Heteractis magnificalis* (HMGs). *Toxicon* 51, 1374–1382.